Version 1.0, academic year 2008-2009

C4 LABWORK for NANOTECH students

Contactless optical profilometer/vibrometer

Davide Bucci, Bogdan Bercu, Quentin Rafhay

Introduction

This labwork will be dedicated to the study of the surface topography and vibrational properties of microelectronic circuits as well as Micro Electro Mechanical Systems (MEMS).

The first part of this document presents the technical background of several characterization techniques, all based on a contactless optical interferometric system. The first paragraph thus describes the Michelson interferometer, which is the basis of the Fogale ZoomSurf 3D system used in this labwork. Then, we will see how to exploit this interferometric system in order to measure the surface topography and the vibration modes of a Micro Electro Mechanical System (MEMS).

In the second part, questions are provided in order to guide the practical work.

I –Technical background and measurement techniques

1. The Michelson interferometer

Our measurement system is relying on the combined use of optical investigation and interferometry. To understand the working principle, we will begin by considering a classic Michelson interferometric system, as the one depicted in Figure 1.

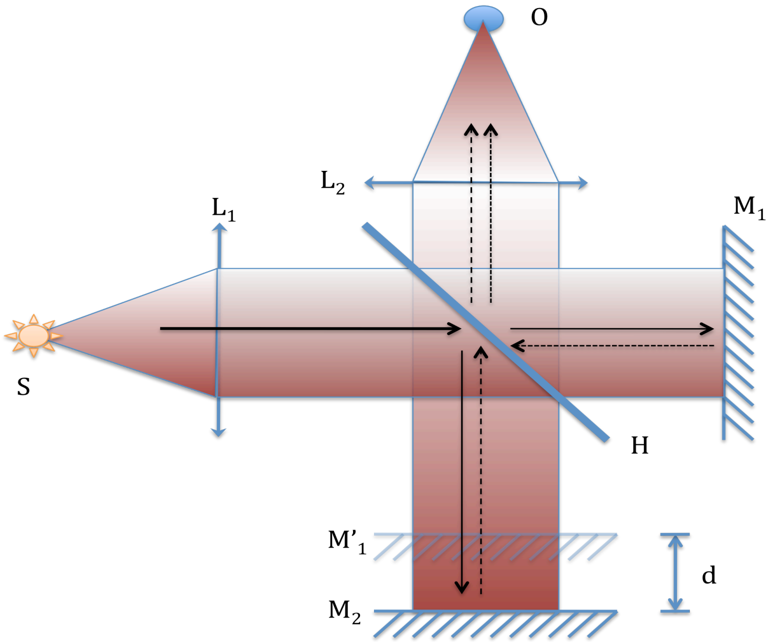

Figure 1: a classic Michelson interferometer

The light beam provided by the source S is collimated by the lens L_1 and split in two beams by the half reflecting plate H. These two beams are then reflected by mirrors M_1 and M_2 and are then recombined and focused on the observer O.
If the light path difference between the position of the two mirrors corresponds to a phase shift which is an integer multiple of 2π, we will obtain a constructive interference and a bright point in O. If the path difference is a half integer multiple of 2π, we will obtain a destructive interference and a dark point in O.
The phase shift $\Delta\phi$ will correspond to the difference of the optical path due to the asymmetry *d* in the length of the two arms of the interferometer and it is thus:

$$\Delta\phi = 2\ d\ n\ 2\pi/\lambda_0$$

Where λ_0 is the wavelength in vacuum and n the refractive index of the light propagating method, which in our case is air, thus leading n not far from 1.
The ability to make interferences when *d* is far from zero depends on the time coherence of the light source. If S is a quasi-monochromatic LASER source, interferences can be obtained for values of |*d*| of several meters or even kilometers. If we are using a red LED, delivering a much broader spectrum, they can be obtained only for |*d*| not exceeding a few micrometers. If we are using polychromatic light such as the one obtained by a white LED, we will obtain interferences only for |*d*| not exceeding a few hundred of nanometers. Figure 2 shows the interference fringes that can be obtained from a monochromatic or a polychromatic spectrum: it can be shown that there is a Fourier transform relationship between the spectrum and the fringes.

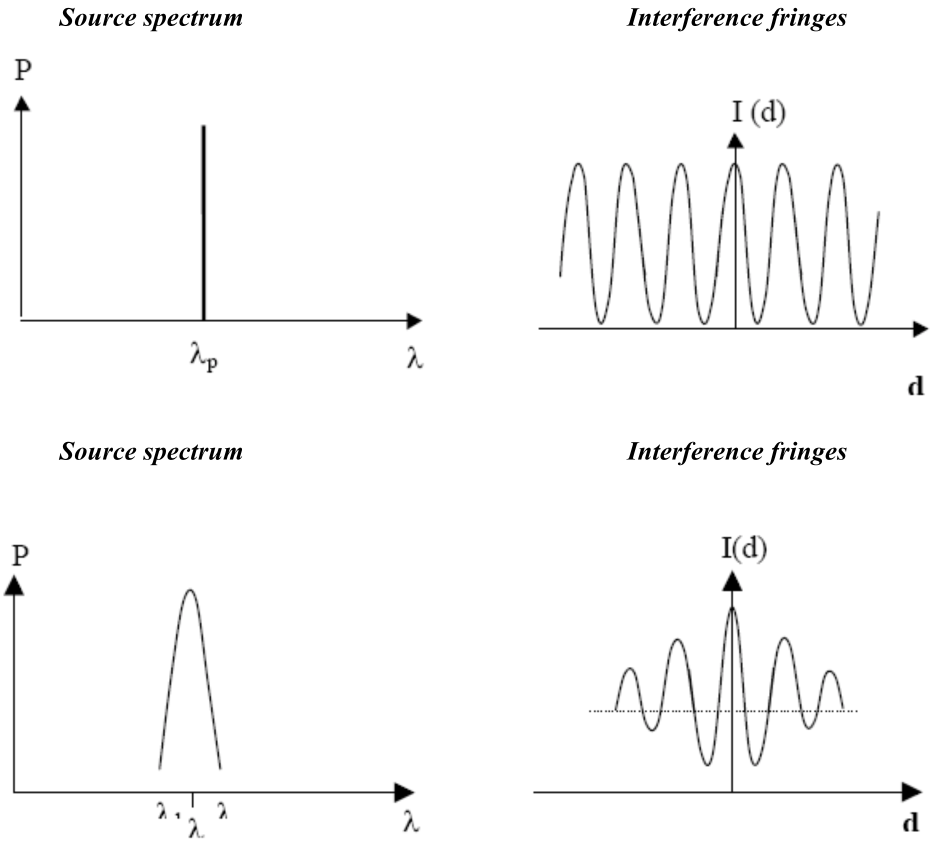

Figure 2: The shape of the interference fringes (right) for a monochromatic source (top) and a polychromatic source (bottom).

A monochromatic light produces constant height fringes while polychromatic light gives a varying envelope, which has a maximum corresponding to a zero difference in the optical paths.

2. The acquisition system "Fogale Nanotech ZoomSurf 3D"

Our goal is to measure the sample topography by means of an optical interferometric system, similar to the Michelson interferometer described above. The main idea depicted in Figure 3 consists in substituting the mirror M_2 with the sample to be characterized, whose surface has been treated in order to be reflective.
The system thus uses a combined principle of interferometry and imaging to obtain a description of the sample.
The L_2 lens is now used to form an image on a CCD camera system and we are able to control very precisely the position of the mirror M_1 by means of a piezo-electric actuator.

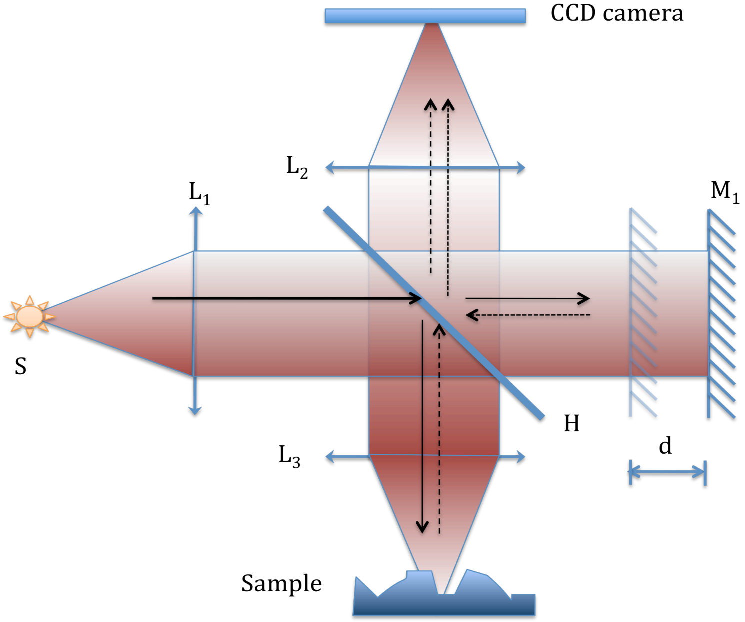

Figure 3: a schematic principle of the ZoomSurf 3D optical profilometer

The optical system is arranged so that each pixel of the CCD camera corresponds to a particular point in the sample surface. By moving the M_1 mirror, we are able to observe the behavior of each point at once on the camera.

The position of the mirror, as well as the light source, is completely controlled by a computer system, which runs the Fogale 3D Pilot software. The same software allows showing on the screen the image captured by the camera and is able to perform image treatments in order to obtain and represent graphically the sample surface topography.

There are two available sources: a red LED and a white LED. The first one will be used as a quasi-monochromatic light source, while the second will be used as a polychromatic source. Since the principles and algorithms involved in the two cases differ, we will describe them separately.

3. Sample topography using white light measurements

In the case of white light measurements, we will use a polychromatic source, which means that its time coherence is weak and it is able to make interferences only when the difference of optical path in the two arms of the interferometer is very small. In this case, we will be able to see interferences whose envelope reaches a maximum if the difference is zero.

Everything works as we had a probing plane that is formed by fringes: only the points of the sample that intersects the probing plane will form interference fringes on the camera image. By moving M_1, we are able to move the position of the probing plane and we are able to scan the whole sample surface topography.

The 3D Pilot software is able to find the maximum of the envelope for each position of the mirror, by performing a simple mathematical treatment. If we consider λ as the center wavelength of the light source, we can write the intensity $I(z)$ of the interference fringes in a (x, y) point as a function of the elevation z:

$$I(z)=A(z-z_0)\cos[4\pi n(z-z_0)/\lambda-\varphi]+C$$

where the envelope A(z) function decreases when $|z-z_0|$ increases and z_0 is the elevation of the considered (x, y) point. Thus, in order to determine z_0, we have to find the maximum of the $A(z-z_0)$ function, which will be at $z = z_0$. If we write:

$$I(z) = A(z-z_0)\left[\frac{\exp\left(4\pi i\frac{z-z_0}{\lambda}-i\varphi\right)+\exp\left(-4\pi i\frac{z-z_0}{\lambda}+i\varphi\right)}{2}\right]+C$$

it is possible to accomplish a linear filtering in order to suppress the continuous component of the signal as well as the negative frequencies.

After such a filtering, we obtain the following form (complex analytic signal):

$$I_f(z) = A(z-z_0)\left[\frac{\exp\left(4\pi i\frac{z-z_0}{\lambda}-i\varphi\right)}{2}\right]$$

The modulus of the complex exponential being equal to 1, the search for the maximum of the $I_f(z)$ modulus determines directly the maximum of the $A(z-z_0)$.

Since this algorithm is applied for each pixel, the white light measurements demand a certain amount of processing power, as well as the acquisition of a high number of images while the mirror is displaced. This method is well suit to analyze large scale (up to a few microns) topography variations, but its accuracy and precision are not very high.

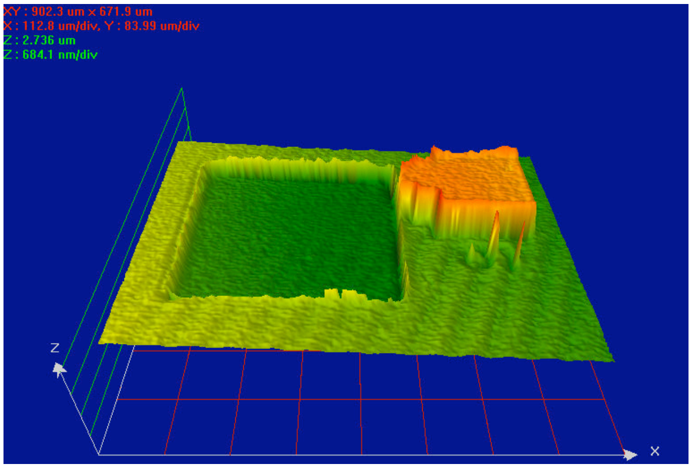

Figure 4: a MOS capacitor topography rendered by the 3D Pilot software

4. Sample topography using monochromatic light measurements

For measuring small roughness or small surface features, another approach can be used, which has been first proposed by P. Carré [1]. If in white light measurements described in section 3 we used the envelope of the interference fringes, in monochromatic light this envelope is a constant. We can in this case exploit the phase term of the interference fringes, which will provide us a nanometric resolution.

This method works well also if we have a not so monochromatic light such as the one provided by a common red LED (λ ≈ 630 nm). In this case, interference fringes can be seen for optical path differences of several tens of micrometers, which is more than we need in practice.

Being positioned at a given *z* position, we acquire four images at the following positions: z, z+δ, z+2δ, z+3δ. The displacement δ is chosen in such a way that the corresponding phase shift $\alpha = 4\pi\delta/\lambda$ is not far from π/2.

Considering a single pixel and supposing that the light source is perfectly monochromatic (which means that the interferogram that we obtain at the considered pixel is nothing more than a raised cosinus) we can write the corresponding light intensities at these four positions:

$$\begin{aligned}
I_1(x,y) &= I_0(x,y)[1+\gamma\cos(\phi(x,y))] \\
I_2(x,y) &= I_0(x,y)[1+\gamma\cos(\phi(x,y)+\alpha)] \\
I_3(x,y) &= I_0(x,y)[1+\gamma\cos(\phi(x,y)+2\alpha)] \\
I_4(x,y) &= I_0(x,y)[1+\gamma\cos(\phi(x,y)+3\alpha)]
\end{aligned}$$

where $I_0(x,y)$ is the mean intensity and γ is the contrast factor.

The modulation in the (x, y) point is given by:

$$\phi(x,y) = \arctan\frac{\sqrt{[3(I_2-I_3)-(I_1-I_4)][(I_2-I_3)+(I_1-I_4)]}}{(I_2+I_3)-(I_1+I_4)}$$

If we apply these formulas in all pixels of the camera, the $\phi(x,y)$ function represents the phase profile, whose values are comprised between 0 and 2π and can be converted into elevation through a λ/2π multiplication.

Sample surface

Sample surface imaged by Carré technique

Figure 5: the effect of phase wraps

Figure 5 shows the effect of phase wraps in the elevation due to the conversion. The elimination of these discontinuities requires an algorithm of phase unwrapping. There are several methods that allow correcting the artifacts produced by this effect.

Three algorithms are available, which are slightly different in their basic principle (detecting the phase discontinuities and interpreting them as continuous surface) and differs mainly by the order of pixel treatment. Two of them (the gradient and the variance algorithms) use a “quality map” computed using the gradient or the variance, respectively. This map is used to determine the regions that have to be corrected. The third algorithm, the Goldstein algorithm, is more complex, using “short circuit” paths in order to avoid regions where the phase is impossible to unwrap.

Measurements using monochrome light are the best solution in terms of speed (only four images to acquire) and resolution (0.1nm in optimum conditions) for surfaces having features less pronounced than $\lambda/2$. It is equally possible to average several shots at each step in order to increase the signal to noise ratio of the final images taken into account during calculations.

Figure 6 shows an example of the measurement of an aluminum layer surface topography, useful to measure its roughness.

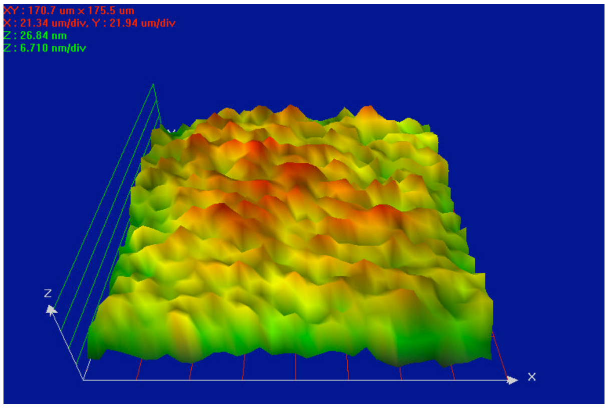

Figure 6: the roughness of an aluminum layer. Note that the *z* scale is 100 times smaller than the one used in Figure 4.

5. Measuring shape and frequency of MEMS vibration modes

The camera used in the acquisition system delivers a standard 25 frames per second (fps) throughput. The standard treatment thus only allows very slow phenomena to be observed, the Nyquist frequency being only 12.5 Hz.

Since MEMS devices often have interesting vibrational properties in the range 1 kHz – 1 MHz, an alternative approach based on the stroboscopic principle has been developed.

The main idea consists in exciting the MEMS under test by means of a piezoelectric actuator at a given frequency. The light source is rapidly switched on and off and delivers short light pulse with a very well controlled phase relationship with the excitation.

By slowly changing the relative phase between the excitation and the pulses, we can analyze very fast phenomena in the camera bandwith. This effect is the same as the one that can be noticed on a car wheel filmed: if the wheel does one turn for each image acquisition it will appear perfectly still in the film.

In other words, in a signal processing point of view, using this method, we are actually undersampling a high frequency but very narrowband phenomenon. The effect of sampling performed by light pulses being to periodize spectrum, we can make a replication of the spectrum fall into the camera bandwidth, thus allowing us to study in detail what it is happening.

A schematic representation of this technique can be seen in Figures 7 and 8, which shows what we would obtain in the case of a pendulum oscillating at high frequency with or without a stroboscopic lightning. If the light is always on, like in Figure 7, the image will appear blurred since the pendulum moves too fast. If short light pulses are synchronized to the pendulum position, we are able to "freeze" the pendulum movement and analyze it with our 25 fps camera system.

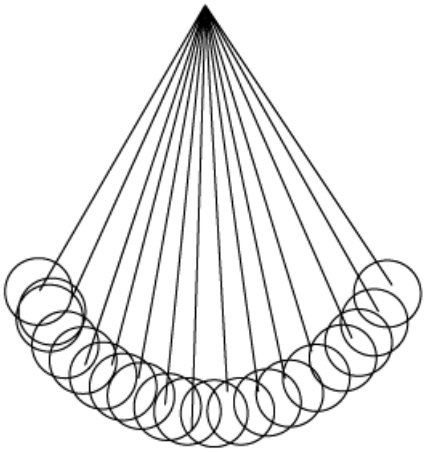

Figure 7: Recording in continuous illumination of a pendulum oscillating at a high frequency compared to the camera bandwidth.

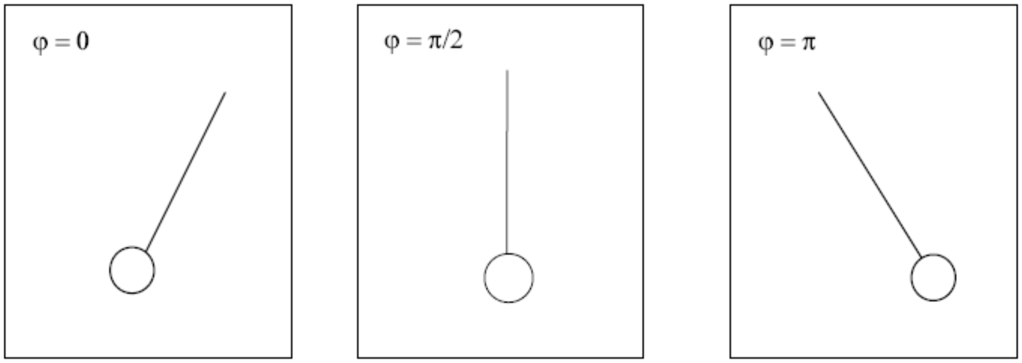

Figure 8: Recording using a stroboscopic illumination synchronous to the pendulum.

Our ZoomSurf 3D system includes a synthesized signal generator, which allows to control the piezo actuator excitation as well as the light source. Figure 9 shows the interface shown by the Pilot 3D software. The first output of the signal generator delivers a sinusoidal signal and will be used for the actuator, while the second output is configured as a pulse generator and will be used for the LED control.

The software can be configured to search for a resonance mode of a MEMS by scanning a particular frequency range, while recording the amplitude of the displacement in one point of the structure (on Pilot 3D: “Spectre de fréquences” menu). Once the resonances have been found, it is interesting to visualize them (“Mésure automatique de phase et d’amplitude” menu). In this case, the excitation frequency is fixed and the software controls the phase between the excitation and the light pulses. A result obtained with this technique is shown in Figure 10, which can be seen animated on the computer.

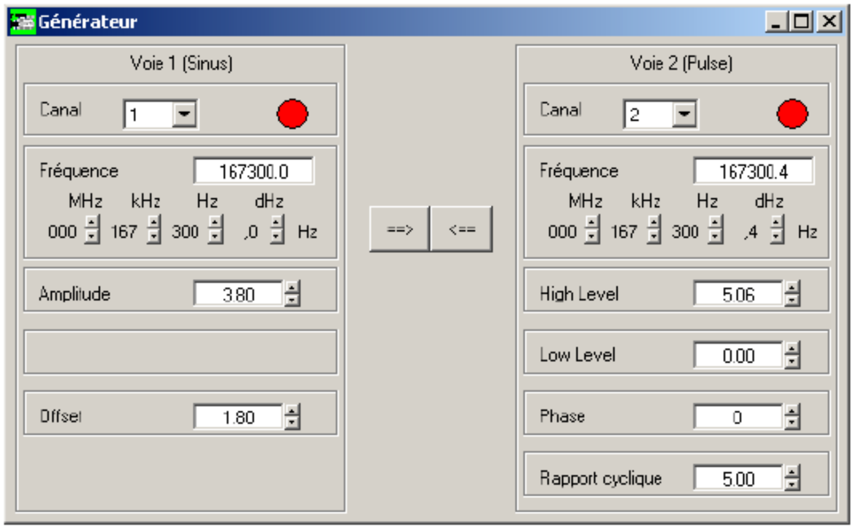

Générateur

Voie 1 (Sinus)

Canal 1

Fréquence 167300.0

MHz kHz Hz dHz

000 167 300 ,0 Hz

Amplitude 3.80

Offset 1.80

Voie 2 (Pulse)

Canal 2

Fréquence 167300.4

MHz kHz Hz dHz

000 167 300 ,4 Hz

High Level 5.06

Low Level 0.00

Phase 0

Rapport cyclique 5.00

Figure 9: the Pilot 3D interface to the double signal generator

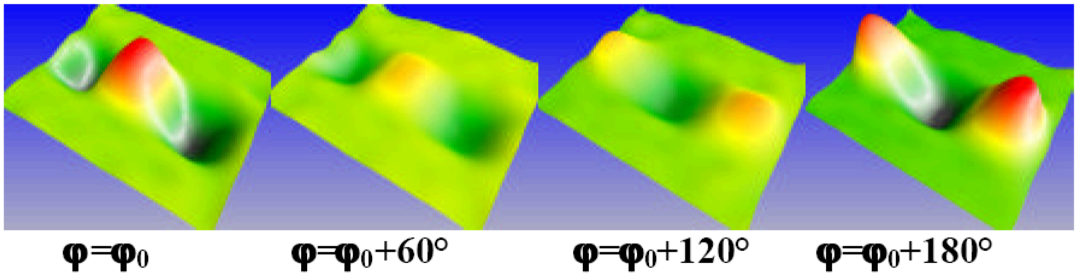

Figure 10: graphical representation of a vibration mode of a membrane. ϕ is the phase difference between the excitation and the stroboscopic illumination

II – Work to be done

Each group of students should provide a short report (not more than 4 pages, not counting figures), two weeks after the labwork session. The report should contain a short description of the measurement techniques, their limitations, as well as a description of the measurements made on the samples. Teachers will evaluate the report and the attitude of each student during the lab session.

1. White light measurements (white LED)

1.1 We will begin by inspecting a processed wafer, which has been previously covered by a thin layer of aluminium. Regulate the focus in order to find interference fringes and, after selecting a small flat region of the sample, use the Pilot 3D software to obtain the source spectrum. What can be said about it?

1.2 Choose an interesting structure to inspect, record its topography, describe and comment it. The software is able to perform automatic tilt compensation as well as apply a selected amount of filtering. Use these tools, if you judge them useful.

1.3 What would happen if we try to characterize a sample which has not been previously prepared? Try to make an example of measurement on such kind of sample and compare it with the results obtained in the question 1.1. What conclusion can be drawn?

1.4 Try to measure the thickness of interesting layers present in your sample. If data about their fabrication is available, for example, from other labworks you have followed, try to make a link between them.

1.5 Try to show the deformation of the silicon membrane in your MEMS sample for example with or without the vacuum sample holding system.

2. Monochromatic light measurements (red LED)

2.1 Obtain the source spectrum and comment it.

2.2 With a certain amount of tilt, compare the rough extracted phase with the unwrapped height results. Compensate as well as you can the tilt between the sample and the interferometer.

2.3 We want to inspect the surface roughness of different layers. In your sample, try to compare for example the roughness of aluminium and silicon dioxide. Comment about the origin of the measured roughness.

3. Vibration modes of an AFM 450 µm cantilever

In this part, we will inspect the resonance modes of an AFM cantilever excited by a piezoelectric actuator. Figure 11 shows the simulated shape of the first resonance mode of the cantilever, while figure 12 shows the second and third mode.

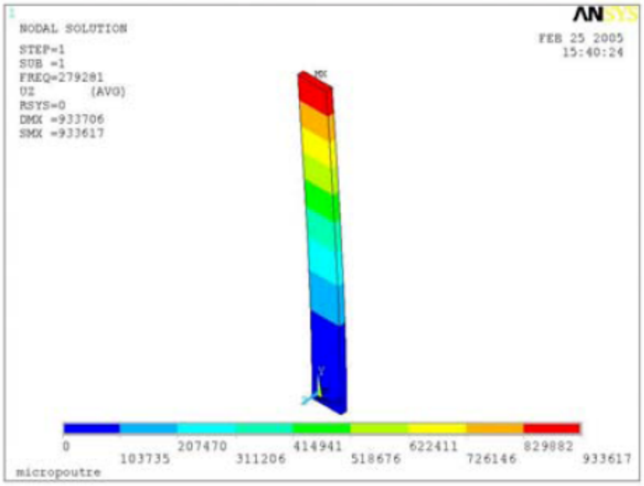

Figure 11: shape of the first resonance mode of the cantilever

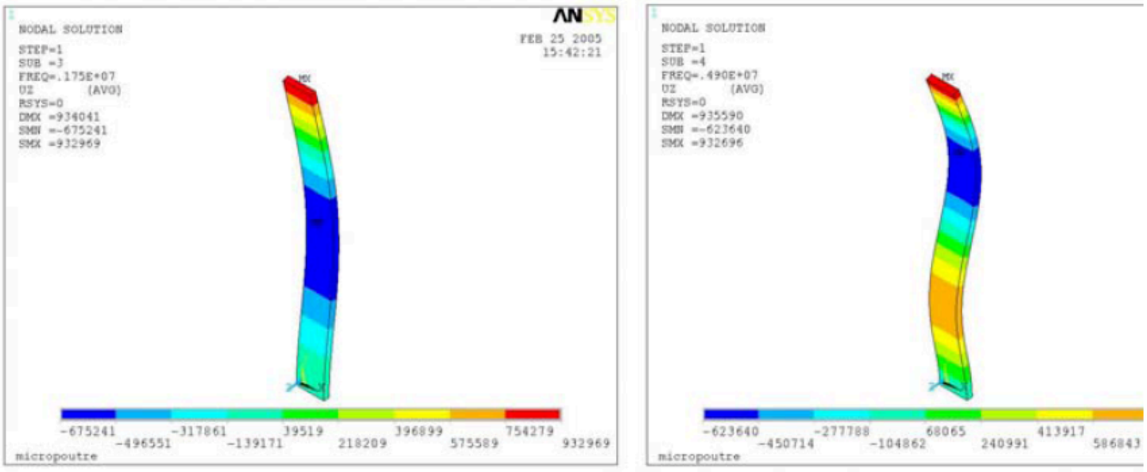

Figure 11: shape of the second and third resonance mode of the cantilever

It can be shown that the fundamental frequency can be obtained using the following expression:

$$f_0 = \frac{1}{2\pi}\sqrt{\frac{EH^2}{4L^4\rho}} \qquad (3.1)$$

In the particular case of this AFM cantilever made by mono crystalline silicon, the material and geometrical values to be used are: Young modulus E=165 GPa, cantilever length L=450 µm, density ρ=2300 kg/m^3. H represents the cantilever thickness.

In the case of the clamped beam, it can be shown that the eigenfrequencies corresponding to the superior modes can be approximated in the following way:

$$f_n = \frac{f_0}{\sqrt{12}}(k_n L)^2 \cong \frac{f_0}{\sqrt{12}}\left[\left(n-\frac{1}{2}\right)\pi\right]^2 \qquad (3.2)$$

where k_n is given by the characteristic equation: $1+\cos(k_n L)\cosh(k_n L) = 0$ (resulting from the boundary conditions).

3.1 Mount the AFM tip on its holder and configure the system in order to use a red light source. Try to obtain fringes on the top of the cantilever.
3.2 Find the vibration mode of your AFM tip by sweeping the excitation frequency. For a 450 µm tip, we have something interesting around 12 kHz. What observation can be done concerning the choice of the analyzed region for this measurement?
3.3 Using expression (3.1), evaluate the thickness of the cantilever. Try to guess the frequencies of the second and third vibration modes.
3.4 Place yourself on the interesting resonant frequencies of the structure. Record and visualize vibration modes. Comment the results obtained.

III – Bibliography

[1] P. Carré, “Installation et utilisation du comparateur photoélectrique et interférentiel du Bureau International des Poids et Mesures”, Metrologia 13-23 (1966)